HUMID ENVIRONMENT STABILITY OF LPCVD ZNO:B USED AS TRANSPARENT ELECTRODES IN THIN FILM SILICON SOLAR CELLS

Jérôme Steinhauser[1], Stefan Meyer[1], Marlène Schwab[1], Sylvie Faÿ[1], Christophe Ballif[1], U. Kroll[2], and D. Borrello[2]

[1]Institute of Microtechnology (IMT), university of Neuchâtel, CH-2000 Neuchâtel, Switzerland.

[2] Oerlikon Solar-Lab, 2000 Neuchâtel, Switzerland.

ABSTRACT

The stability in humid environment of low pressure chemical vapor deposited boron doped zinc oxide (LPCVD ZnO:B) used as transparent conductive oxide in thin film silicon solar cells is investigated. Damp heat treatment (exposition to humid and hot atmosphere) induces a degradation of the electrical properties of unprotected LPCVD ZnO:B layers. By combining analyses of the electrical and optical properties of the films, we are able to attribute this behavior to an increase of electron grain boundary scattering. This is in contrast to the intragrain scattering mechanisms, which are not affected by damp heat exposure. The ZnO stability is enhanced for heavily doped films due to easier tunneling through potential barrier at grain boundaries.

1. INTRODUCTION

Transparent conducting oxide (TCO) films with a high electrical conductivity combined with a high transparency are required as transparent electrode layers in thin film silicon solar cells. The Institute of Microtechnology (IMT) of Neuchâtel develops Boron doped zinc oxide (ZnO:B) layers fabricated by Low pressure chemical vapor deposition (LPCVD) [1]. This material is particularly well suited as electrodes in thin film silicon amorphous and micromorph solar cells because, in addition to good transparency and conductivity properties, it possesses an as grown capacity to scatter the light. Scattering the light at the TCO-cell interface increases the effective absorption of light within the active layer of the solar cells leading to device with higher current [2,3]. This light scattering effect can be obtained with TCO having important surface roughness. LPCVD ZnO:B layers are polycrystalline and are constituted of grains with the (11-20) crystallographic plans parallel to the substrate. As shown in figure 1, the extremities of these grains appear at the growing surface as large pyramids, which yield in an as grown rough surface texture that efficiently scatter the light. LPCVD ZnO:B layers is already used as electrodes in large area solar modules [4]. Solar modules intended to be commercially distributed are submitted to standard stability test [5] like damp heat exposure. Several authors [6,7] have observed that ZnO films can show a degradation of their electrical properties after damp heat treatment. Even if encapsulated modules using LPCVD ZnO:B layers have been shown by Kroll et al. [2] to successfully pass the standard damp heat test (exposure to 85% humidity at 85°C during 1000 hours), it is important to understand the stability behavior of LPCVD ZnO:B films in a humid environment as these properties will dictate some of the requirements on the encapsulation. ZnO film stability improvements can even lead to relaxed requirements. In this contribution, the degradation of the electrical film properties due to damp heat treatment without any encapsulation is analyzed. We discuss the possible mechanisms explaining the damp heat behaviors of LPCVD ZnO:B layers

with various carrier density. Finally, we demonstrate that unencapsulated solar cells stable during damp heat can be achieved using LPCVD ZnO:B layers as electrodes.

2. EXPERIMENTAL

LPCVD ZnO:B layers are deposited at low temperature (below 200°C) on 0.7 mm thick Schott AF45 glass substrates. Diethylzinc (DEZ) and water vapor are used as precursors and directly evaporated in the system. DEZ and H_2O flows are set to 13.5 sccm and 16.5 sccm, respectively. Diborane (B_2H_6) diluted 1% in argon is used as doping gas. The thickness of the layers, measured with a stylus profilometer, is 2 μm. LPCVD ZnO:B samples with three different doping levels are studied. They are labeled "lightly", "standard" and "heavily" doped. The gas phase doping ratio ($[B_2H_6]/[DEZ]$) used during the ZnO deposition is equal to 0.3, 0.6 and 2 for lightly, standard and heavily doped samples, respectively.

State of the art single-junction aSi:H solar cells are deposited in pin configuration. Two batch of cells are fabricated, one using standard LPCVD ZnO:B and one using heavily doped LPCVD ZnO:B as front and back electrodes. The cells are deposited in Oerlikon KAI-S R&D deposition systems at an excitation frequency of 40.68 MHz. The solar cells are fully patterned with areas of 0.25 cm^2. The thickness of the intrinsic layer is about 250 nm.

After deposition, non encapsulated ZnO films and solar cells are exposed to damp heat atmosphere with 100 % relative humidity at a temperature of 40 °C or 80°C for up to 800 hours. These conditions are different from the standardized damp heat test (85 °C, 85 %

humidity) to slow down the degradation kinetics (for measurements at 40°C) in order to precisely record the changes in the electrical characteristics of the films, or for experimental simplicity (humidity at 100% instead of 85%). We measure the electrical characteristics of the samples initially and for different damp heat exposure duration.

The resistivity ρ, the Hall carrier concentration N_{Hall}, and the Hall mobility μ_{Hall} are deduced from Hall effect measurement with an HEM-3000 Hall system using a Van der Pauw configuration at room temperature.

We measure the temperature dependence of the conductivity (σ) using a four-probe configuration. We place the samples in a cryostat cooled with liquid helium. The temperature is precisely controlled with a heater using a feedback loop based on an in situ temperature sensor measurement. A Keitley 2600 sourcemeter executes a current voltage measurement during a temperature ramp from 300 K to 30 K.

A 1720X Perking-Elmer FTIR spectrometer with a reflectance accessory is used to measure the reflectance spectra in the infrared (IR) region. The Drude dielectric function $\varepsilon(\omega) = \varepsilon_\infty - (\omega_N^2/(\omega^2 + i\Gamma\omega))$ is well suited to describe the IR optical properties of LPCVD ZnO:B, as shown in [8]. ε_∞ is the high frequency dielectric function assumed equal to 4 for ZnO. Taking into account the multiple reflections due to the air/glass/ZnO/air structure, reflectance spectra calculated using the Drude model, with the unscreened plasma frequency ω_N and the Drude damping factor Γ as fitting parameters, are fitted to the experimental measured reflectance spectra. Taking the values of ω_N and Γ extracted from the best reflectance fit, the optical carrier concentration N_{optic} and mobility μ_{optic} are then deduce using $N_{optic} = \omega_N^2\varepsilon_0 m^*/e^2$ and $\mu_{optic} = e/\Gamma m^*$, where e is the electron charge, ε_0 the

permittivity of free space and m* the electron effective mass assumed equal to $m^* = 0.28m_e$ for ZnO, m_e is the electron mass. The optically deduced electrical parameters and the electrical parameter measured by Hall effect are influenced by different scattering mechanisms. The electron mean free path in ZnO is in the range of a few nm and, with the application of a rapidly oscillating electric field (i.e. under NIR light excitation) the average electron path length remains much smaller than the typical grain size. Note that the grain boundaries occupy only a small volume compared to the bulk of the grain and, hence, are considered as not affecting the optical measurements. Therefore, grain boundary scattering will not influence the measured value for the optical mobility, and only intra-grain scattering will influence μ_{optic}. In the case of the Hall effect measurement, electrons have to travel over a macroscopic length (across several grain boundaries) and consequently both intra-grain scattering and grain boundary scattering will influence the measured value of μ_{Hall} [8].

Electrical characteristics of the solar cells are obtained from current-voltage measurements measured under a WACOM solar simulator in standard test conditions (25 °C, AM1.5g spectrum, and 1000 W/m^2). The cells are measured without white dielectric back reflector, which explains the moderate values of the cell short circuit-current.

3. RESULTS AND DISCUSSION

Figure 2, 3 and 4 show the resistivity, the optical and Hall mobility, and the optical and Hall carrier density, respectively, as a function of the damp heat exposure time for the standard LPCVD ZnO:B film. The initial Hall and optical carrier density, N_{Hall} and N_{optic}, are identical

equal to ~1×10^{20} cm^{-3}. The initial Hall and optical mobility, μ_{Hall} and μ_{optic}, are close equal to 33 and 36 $cm^2V^{-1}s^{-1}$, respectively. These values correspond to an initial resistivity of about $\rho = 2.2\times10^{-3}$ Ω.cm. After 800 hours of damp heat exposure, the resistivity of the film increases from 2.2×10^{-3} to 4.6×10^{-2} Ω.cm. This increase is mainly due to a sharp drop of the Hall mobility, which decreases from 33 to 2 $cm^2V^{-1}s^{-1}$, whereas the Hall carrier density is only slightly affected. Optical values μ_{optic} and N_{optic} remain constant after 800 hours of damp heat exposure.

A similar damp heat degradation behavior was observed in sputtered ZnO:Al films by several authors [6, 9-11]. They explained the degradation of the electrical property of ZnO layers by diffusion of environmental gases or molecules like oxygen, carbon dioxide and water vapor into the films. Pern [9] considers hydratation/hydrolysis reaction at weak defects that cause discontinuity of the electrical path. Beyer [11] discusses ZnO as a highly compact material with little in and out-diffusion up to 1000°C of atoms or molecules with sizes >Ne, and concludes, in accordance with Lin [10], that environmental gases or molecules diffuse via defect path (i.e. grain boundary). However, in these works, no clear separation between grain boundary and intragrain scattering is performed. In constrat, for our LPCVD ZnO:B films, the observed difference between optical mobility and Hall mobility values gives a first direct evidence of an increasing grain boundary electron scattering with the increasing damp heat exposure duration.

As described by Seto in the case of polycrystalline silicon [12], we can consider in LPCVD ZnO:B polycrystalline films trap states localized in the grain boundaries, which captures electrons from the conduction band. The grain boundaries are charged negatively and a space charge region extends into the crystallite forming a "back-to-back" schottky potential

barrier [12,13]. LPCVD ZnO:B films are heavily doped, degenerate, semiconductor, thus the barrier are relatively low and narrow . Considering a carrier density $N = 10^{20} cm^{-3}$ and a trap density $N_t = 10^{13}$ cm^{-2}, the barrier width, given by $W = N_t/N$ is equal to 1 nm and the barrier height $eV_b = (e^2 N_t^2)/(8\varepsilon\varepsilon_0 N) = 28$ meV where ε is the dielectric permittivity of the material (here we take $\varepsilon = 8.12$), ε_0 is the dielectric permittivity of free space and e is the electron charge. With such low values of W and eV_b tunneling can be consider as a possible current path. In figure 5, the conductivity as a function of the inverse of the temperature is shown for the standard LPCVD ZnO:B sample after varying damp heat exposure times. The shape of the $\sigma(T^{-1})$ curves around ambient temperature changes while the damp heat exposure time is increased. The conductivity decreases with the inverse of the temperature for non degraded samples and starts to increases with T^{-1} for longer damp heat exposure. For non damp heat treated LPCVD ZnO:B, tunneling can be considered as the dominant current path trough the grain boundary potential barrier as indicate by the weak dependence of the conductivity with the temperature and the high conductivity at low temperature. As the damp heat time increases, the experimental curves of the conductivity as a function of the temperature show an increasing dependence with the temperature and a reduce conductivity at low temperature. This dependence with the temperature indicates a transition toward a more thermionic emission-like governed conductivity. We can explain this behavior by diffusion of water vapor at grain boundaries that lead to an increase of the trap state density, and thus to higher and wider potential barrier. Therefore the current path through the barrier by tunneling is reduced and thermionic emission contributes primarily to the transport. Figure 6 shows a schematic diagram that illustrates these mechanisms. For the considered range of doping and defect densities, it is likely that a thermionic field-emission effect, including a tunneling effect at

higher electron energies, governs the T behavior, rather than a pur thermionic emission [14].

Figure 6 shows the resistivity as a function of damp heat exposure duration for a lightly doped (N = 3×10^{19} cm^{-3}), a standard doped (N = 1×10^{20} cm^{-3}) and an heavily doped (N = 3×10^{20} cm^{-3})LPCVD ZnO film. This figure shows that films with lower doping level are less stable against damp heat exposure. We strongly enhance the stability as we increase the doping level in the LPCVD ZnO:B films. The stability differences between samples with different doping levels can also be explained by increasing charge states at grain boundaries during damp heat. A heavier doping of the ZnO grains reduces the width W and the height eVb of the the grain boundary barrier to small values even with a high density of trap states (typically W < 3 nm and eV_b < 350 meV for N = 2 10^{20} cm^{-3} and N_t < 5 10^{13} cm^{-2}). These small values of W allow an important current path via tunneling through the potential barriers and thus more stable films.

Figure 7 and 8 show the current-voltage characteristics of solar cells deposited with “standard” and heavily doped LPCVD ZnO:B as both front and back electrodes for various damp heat exposure time (80°C, 100% humidity, without encapsulation). After damp heat exposure, the solar cell deposited with the standard LPCVD ZnO:B as electrodes shows strongly degraded electrical characteristics due to an increase of the serial resistance of the cell. The fill factor (FF) of the cell decrease from 74 % to 28 % after 648 hours damp heat exposure, leading to an efficiency decrease from 9.4 % to 2.8 %. The solar cell with heavily doped LPCVD ZnO:B as electrodes shows slight changes in is current-voltage characteristics after damp heat exposure. The FF varies from 76 % to 70 % and the efficiency slightly decreases from 8.2% to 7.4 % after 648 hours damp heat exposure.

Figure 8 reveals the remarkable stability during damp heat treatment of unprotected aSi:H solar cells using heavily doped ZnO:B layers as electrodes compare to the cells using standard ZnO:B layers. This results demonstrates the possibility to easily achieved more stable cells using heavily doped LPCVD ZnO:B as TCO, implying potential lower requirements for the encapsulation of solar modules.

4. CONCLUSION

LPCVD ZnO:B films show an increase in resistivity during humidity exposition of the unprotected layers, mainly due to a decrease of the Hall mobility, in contrast to the carrier density and optical mobility which remain stable. The temperature dependence of the conductivity shows a more and more thermionic-like behaviour with the increasing damp heat exposure time. These results demonstrate that potential barriers at grain boundaries increase after damp heat exposure leading to higher electron scattering, in contrary to intragrain scattering which remains stable. This phenomenon can be explained by diffusion of water vapor that increases the trap state density at grain boundary. We obtain more stable films by increasing the carrier density due to an enhanced tunnelling trough the potential barriers at grain boundary even if the trap density is high. Finally we show that unencapsulated solar cells using heavily doped LPCVD ZnO:B as electrodes have remarkable stable behaviour during damp heat exposure tests.

REFERENCES

[1] S. Faÿ, L. Feitknecht, R. Schlüchter, U. Kroll, E. Vallat-Sauvain, A. Shah, *Solar Energy Materials and Solar Cells* **90**, 2960 (2006).

[2] A. Shah, J. Meier, A. Bucechel, U. Kroll, J. Steinhauser, F. Meillaud, H. Schade, and D. Dominé, *Thin Solid Films* **502**, 292, (2006).

[3] J. Müller, B. Rech, J. Springer, and M. Vanecek, *Solar Energy Materials and Solar Cells* **77**, 917, (2004).

[4] J. Meier et al. *Proceedings of the 23th European Photovoltaic Solar Energy Conference*, Dresden, Valencia, Spain, (2008).

[5] U. Kroll, J. Meier, S. Benagli, T. Roschek, J. Spitznagel, A. Huegli, D. Borello, M. Mohr,O. Kluth, D. Zimin, G.Monteduro, J. Springer, G. Androutsopoulos, C. Ellert, W. Stein, G. Buechel, A Zindl, A. Buechel, D. Koch-Ospelt, *Proceedings of the 21st European Photovoltaic Solar Energy Conference*, Dresden, Germany, 1551, (2006).

[6] T. Tohsophon, J. Hüpkes, S. Calnan, W. Reetz, B. Rech, W. Beyer, N. Sirikulrat, *Thin solid films* **511**, 673 (2006).

[7] B. Sang, K. Kushiya, D. Okumura, O. Yamase, *Solar Energy Materials and Solar Cells* **67**, 237 (2001).

[8] J. Steinhauser, S. Faÿ, N. Oliveira, E. Vallat-Sauvain, C. Ballif, *Appl. Phys. Letters* **90**, 142107 (2007).

[9] F.J. Pern, B. To, C. Dehart, X. Li, S.H. Glick and R. Noufi, *Proceedings of SPIE*, the International Society for Optical Engineering **7048**, 70480P.1 (2008).

[10] W. Lin, R. Ma, J. Xue, and B. Kang *Solar Energy Materials and Solar Cells* **91**, 1902 (2007).

[11] W. Beyer, J. Hüpkes, H. Steibig, *Thin solid films* **516**, 147 (2007).

[12] J.Y. Seto, *Journal of Applied Physics* **46**, 5247, (1975).

[13] J.W. Orton, *Thin solid films* **86**, 351, (1981).

[14] S.M. Sze, *Physics of semiconductors*, 2nd ed. (John Wiley & Sons) ISBN 0-85226-846-7, 1981.

Figure captions

Figure 1 : Scanning electron micrograph of the surface of a 2 μm thick LPCVD ZnO:B film.

Figure 2 : Resistivity of a 2 μm thick standard doped ($[B_2H_6]/[DEZ] = 0.6$) LPCVD ZnO:B film in function of the damp heat exposure (40°C, 100% humidity) time.

Figure 3 : Optical and Hall mobility of a 2 μm thick standard doped ($[B_2H_6]/[DEZ] = 0.6$) LPCVD ZnO:B film as a function of the damp heat exposure (40°C, 100% humidity) time.

Figure 4 : Optical and Hall carrier density of a 2 μm thick standard doped ($[B_2H_6]/[DEZ] = 0.6$) LPCVD ZnO:B film as a function function of the damp heat exposure (40°C, 100% humidity) time.

Figure 5 : Conductivity as a function of the inverse of the temperature for a 2 μm thick standard doped ($[B_2H_6]/[DEZ] = 0.6$) LPCVD ZnO:B film for various damp heat exposure (80°C, 100% humidity) time.

Figure 6 : Schematic drawing of the current path trough a grain boundary barrier for initial and damp heat degraded LPCVD ZnO:B samples.

Figure 7 : Resistivity as a function of damp heat exposure (80°C, 100% humidity) time for a lightly ($[B_2H_6]/[DEZ] = 0.3$), standard ($[B_2H_6]/[DEZ] = 0.6$) and heavily ($[B_2H_6]/[DEZ] = 2$) doped LPCVD ZnO:B sample.

Figure 8 : Current voltage characteristics of an unencapsulated aSi:H solar cell fabricated with standard doped ($[B_2H_6]/[DEZ] = 0.6$) LPCVD ZnO:B electrodes for various damp heat exposure (80°C, 100% humidity) times.

Figure 9 : Current voltage characteristics of an unencapsulated aSi:H solar cell fabricated with heavily doped ($[B_2H_6]/[DEZ] = 2$) LPCVD ZnO:B electrodes for various damp heat exposure (80°C, 100% humidity) times.

4. Figures (if any)

Click here to download 4. Figures (if any): Fig 1.pdf

Figure 1 :

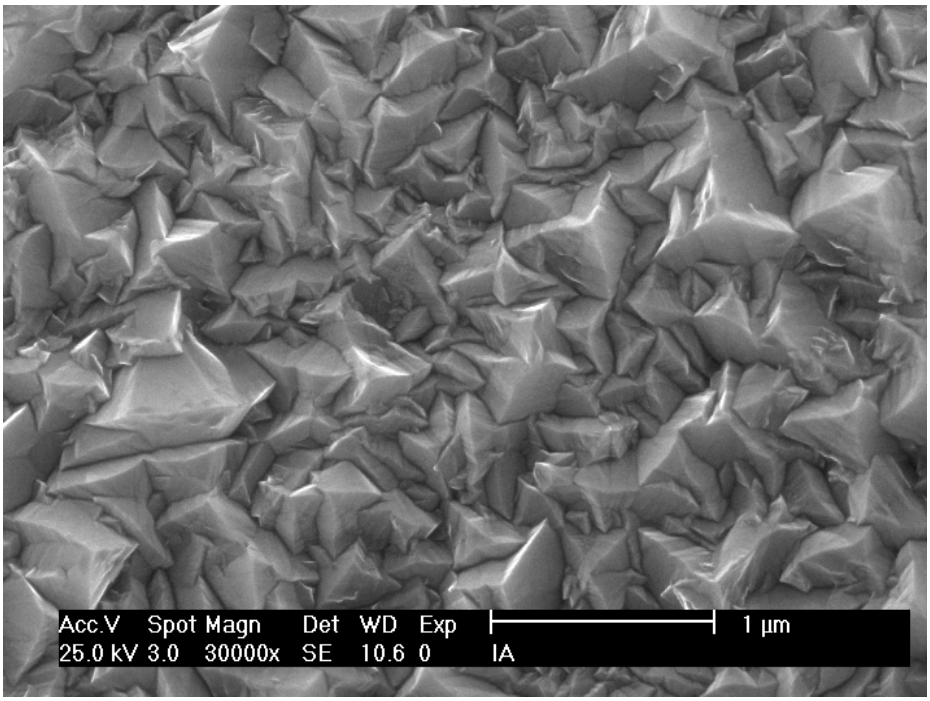

4. Figures (if any)

Click here to download 4. Figures (if any): Fig 2.pdf

Figure 2 :

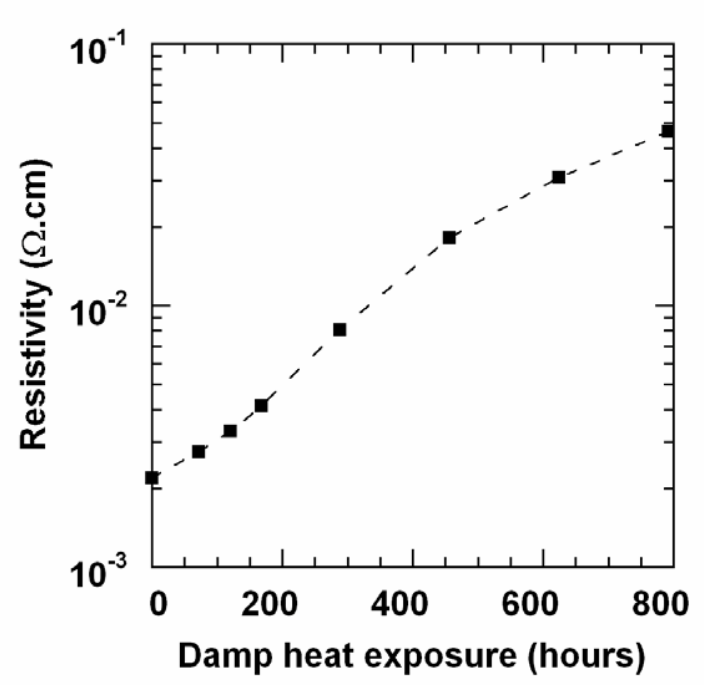

4. Figures (if any)

Click here to download 4. Figures (if any): Fig 3.pdf

Figure 3 :

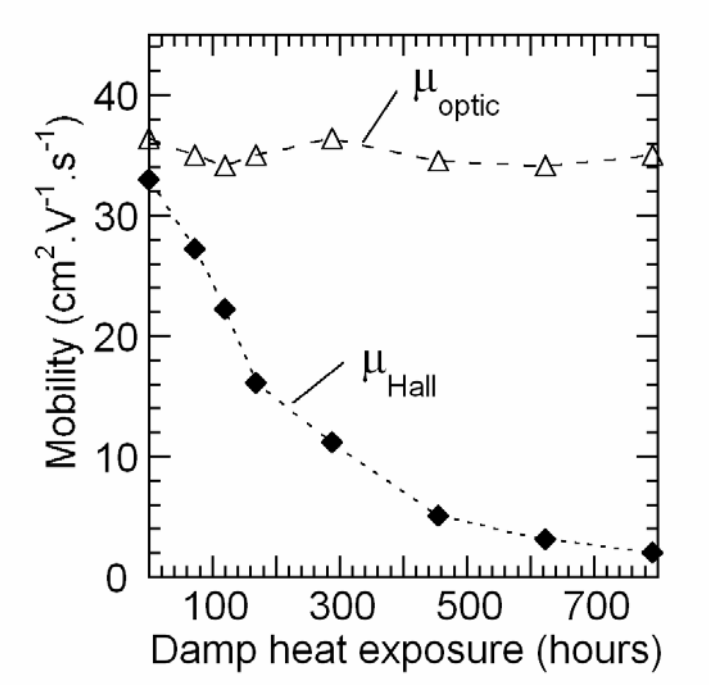

4. Figures (if any)

Click here to download 4. Figures (if any): Fig 4.pdf

Figure 4 :

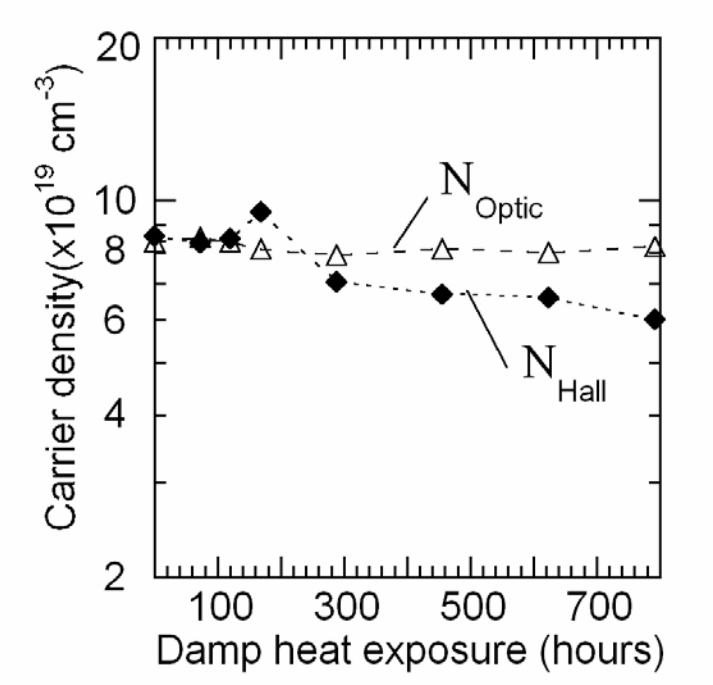

4. Figures (if any)

Click here to download 4. Figures (if any): Fig 5.pdf

Figure 5 :

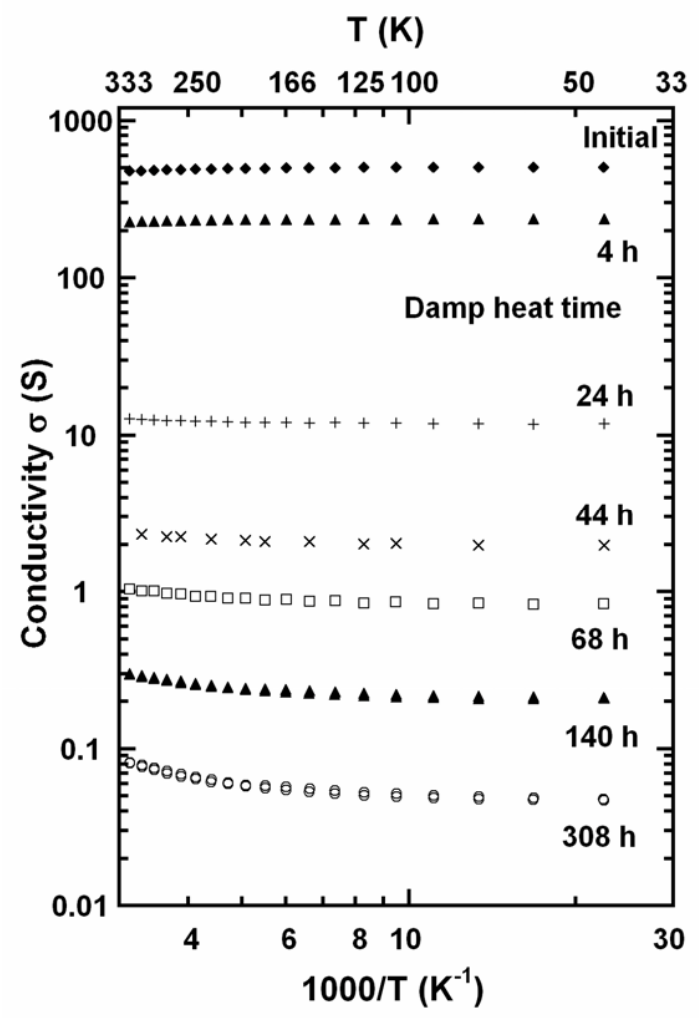

4. Figures (if any)
Click here to download 4. Figures (if any): Fig 6.pdf

Figure 6 :

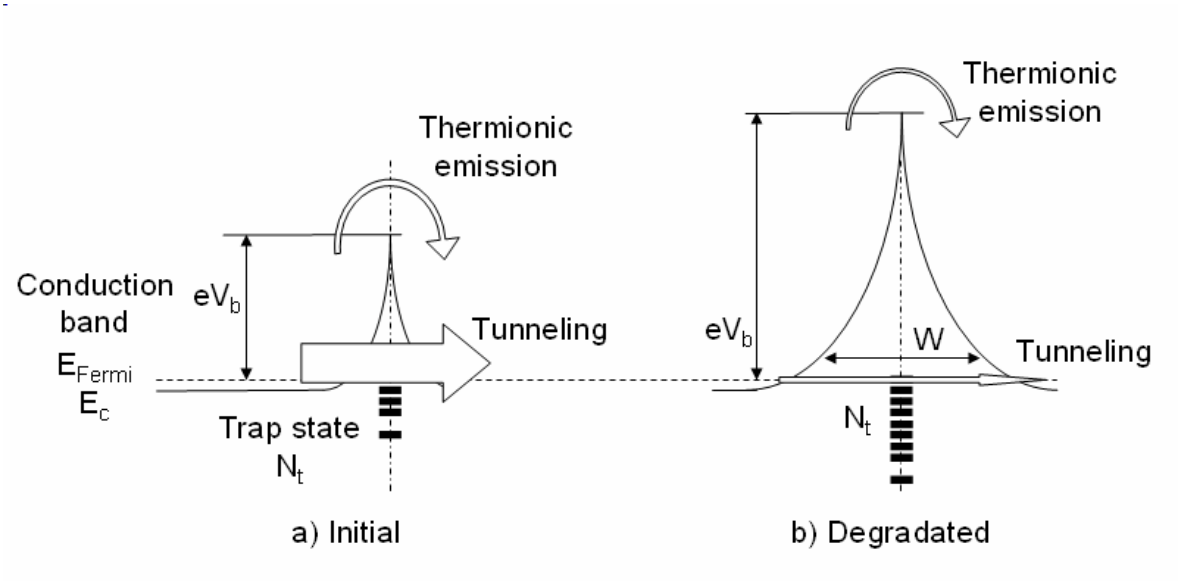

4. Figures (if any)
Click here to download 4. Figures (if any): Fig 7.pdf

Figure 7 :

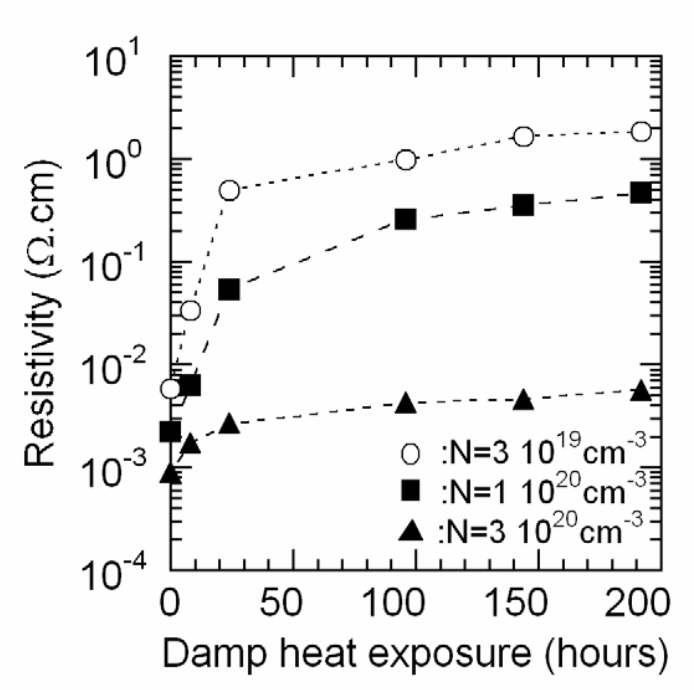

4. Figures (if any)

Click here to download 4. Figures (if any): Fig 8.pdf

Figure 8 :

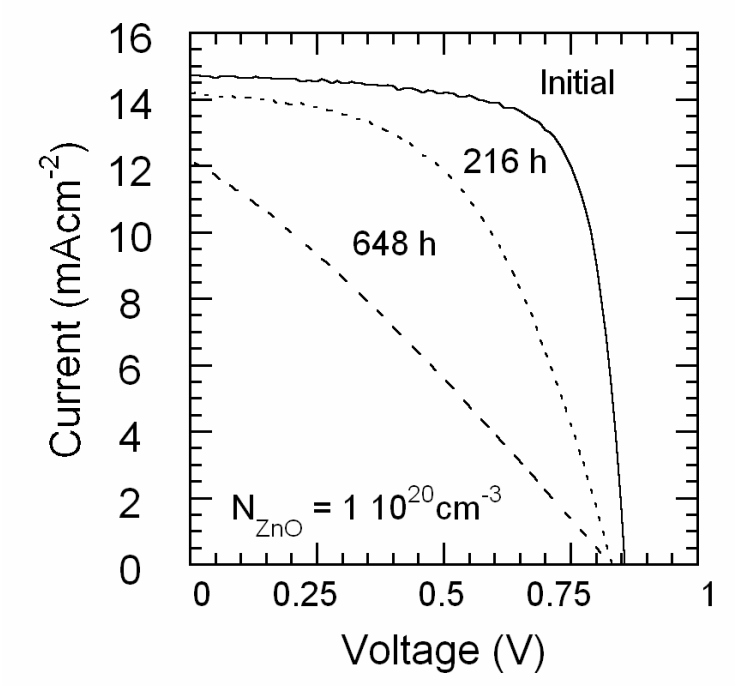

4. Figures (if any)

Click here to download 4. Figures (if any): Fig 9.pdf

Figure 9 :